$BaBi_2O_6$: a Promising n-Type Thermoelectric Oxide with the $PbSb_2O_6$ Crystal Structure — Supplementary Information

Kieran B. Spooner[a],[†,‡] Alex M. Ganose[a],[¶,‡,§] W. W. Winnie Leung,[†] John Buckeridge,[‖,‡] Benjamin A. D. Williamson,[⊥] Robert G. Palgrave,[†] and David O. Scanlon[*,†,‡,§]

†*Department of Chemistry, University College London, 20 Gordon Street, London WC1H 0AJ, UK*

‡*Thomas Young Centre, University College London, Gower Street, London WC1E 6BT, UK*

¶*Department of Materials, Imperial College London, South Kensington Campus, London SW7 2AZ, UK*

§*Diamond Light Source Ltd., Diamond House, Harwell Science and Innovation Campus, Didcot, Oxfordshire OX11 0DE, UK*

‖*School of Engineering, London South Bank University, London SE1 0AA, UK*

⊥*Department of Materials Science and Engineering, Norwegian University of Science and Technology (NTNU), Trondheim 7491, Norway*

E-mail: d.scanlon@ucl.ac.uk

[a]These authors contributed equally to this work.

Convergence

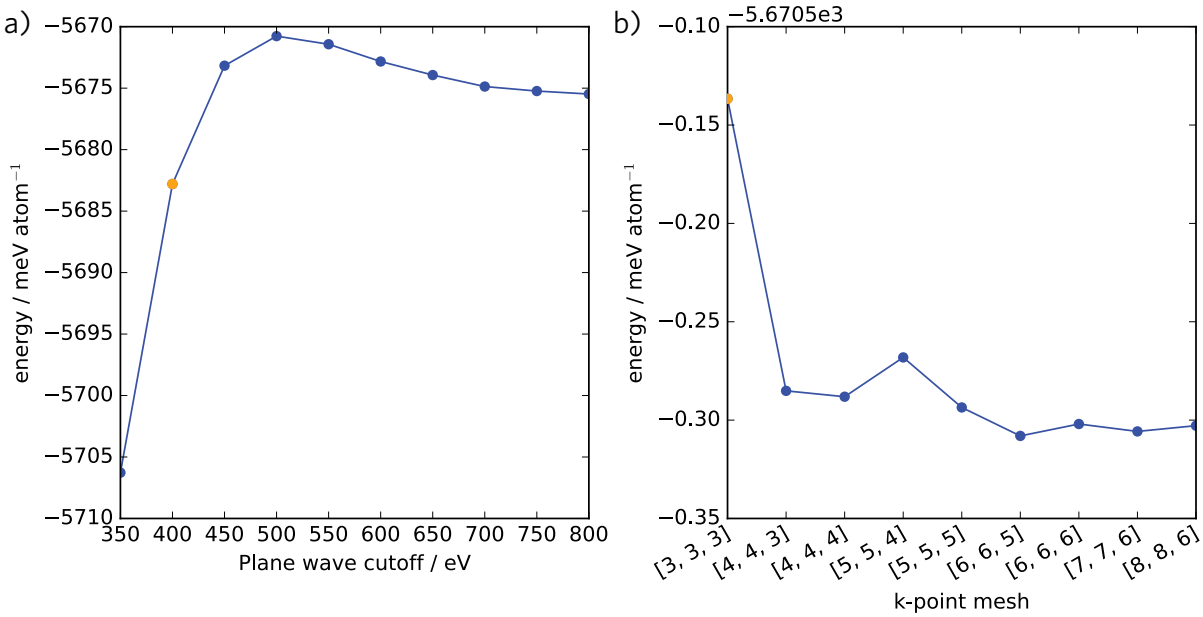

Figure S1: The total VASP energies of $BaBi_2O_6$ against (a) plane-wave energy cut-off and (b) k-point grid. The value converged to 10 meV atom^{-1} is highlighted in orange.

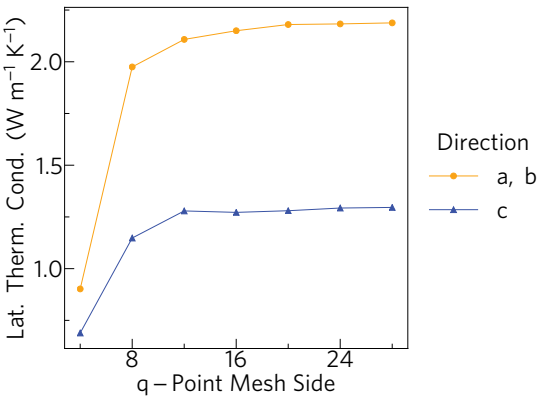

Figure S2: Convergence of the lattice thermal conductivity of $BaBi_2O_6$ against q-point mesh side broken down by lattice direction. Lattice thermal conductivities are converged to 0.01 W m^{-1} K^{-1} by the used $24 \times 24 \times 24$ q-point mesh.

$BaBi_2O_6$ Brillouin Zone

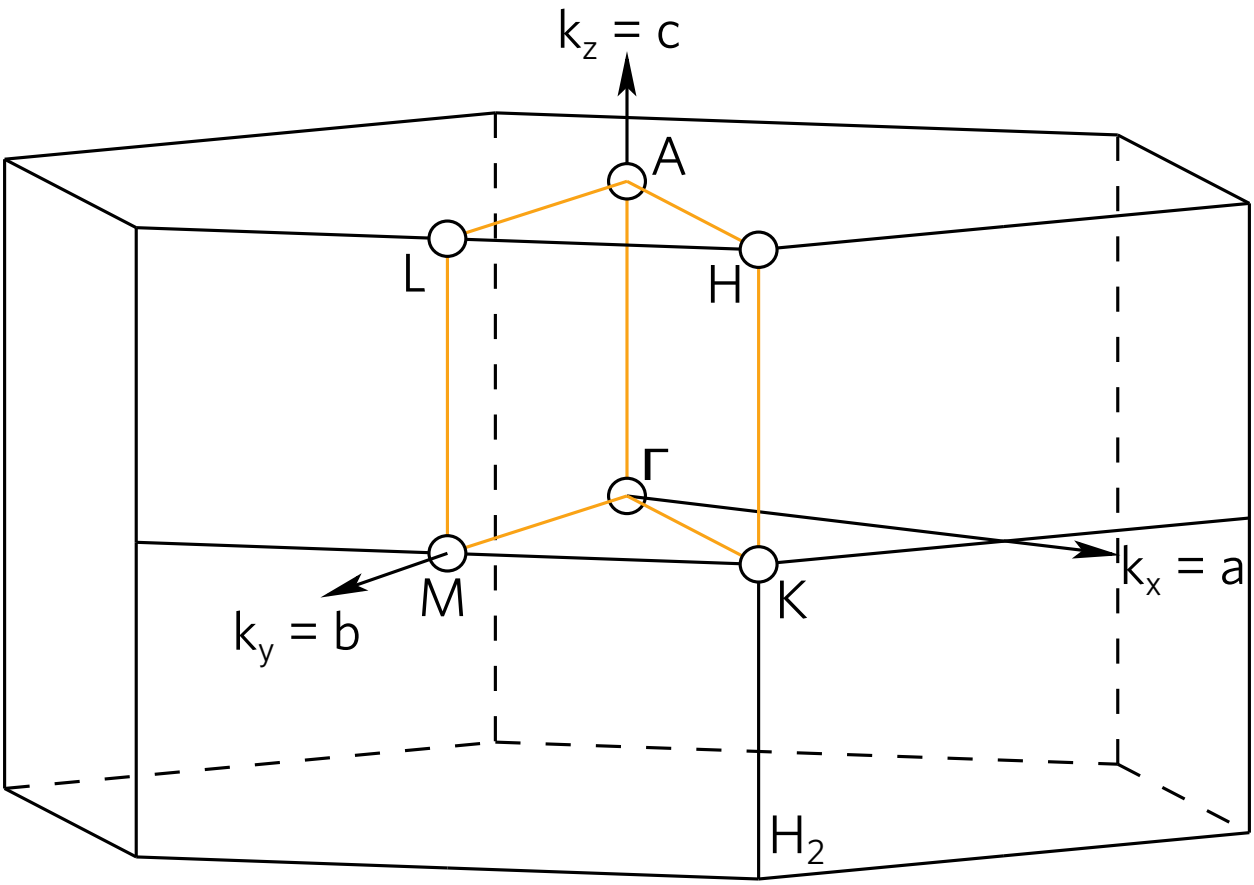

Figure S3: First Brillouin zone of $BaBi_2O_6$ (space group $P\bar{3}1m$ (162)), adapted from the Bilbao Crystallographic Server.[1] The Bradley–Cracknell paths[2] used in the electron and phonon dispersions (main text Figures 5(b) and 8(a)) are shown in orange.

Defects

Table S1: The formation energies of $BaBi_2O_6$ and its competing phases using HSE06

Phase	E_f (eV)
Ba_2Bi_3	-4.363
Ba_4Bi_3	-7.391
BaO	-5.069
BaO_2	-5.736
BiO_2	-2.856
Bi_2O_3	-5.801
Bi_4O_7	-11.71
$Ba_2Bi_2O_5$	-17.26
$BaBi_2O_6$	-12.19

Table S2: The chemical potential limits of the stable region of $BaBi_2O_6$ under O-poor conditions using HSE06, also illustrated in main text Figure 9

Competing Phases		μ_{Ba} (eV)	μ_{Bi} (eV)
Elements	Bi_2O_3	-6.335	-2.927
Bi_2O_3	$Ba_2Bi_2O_5$	-5.398	-2.404
$Ba_2Bi_2O_5$	BaO_2	-5.290	-2.782
BaO_2	Elements	-5.736	-3.227

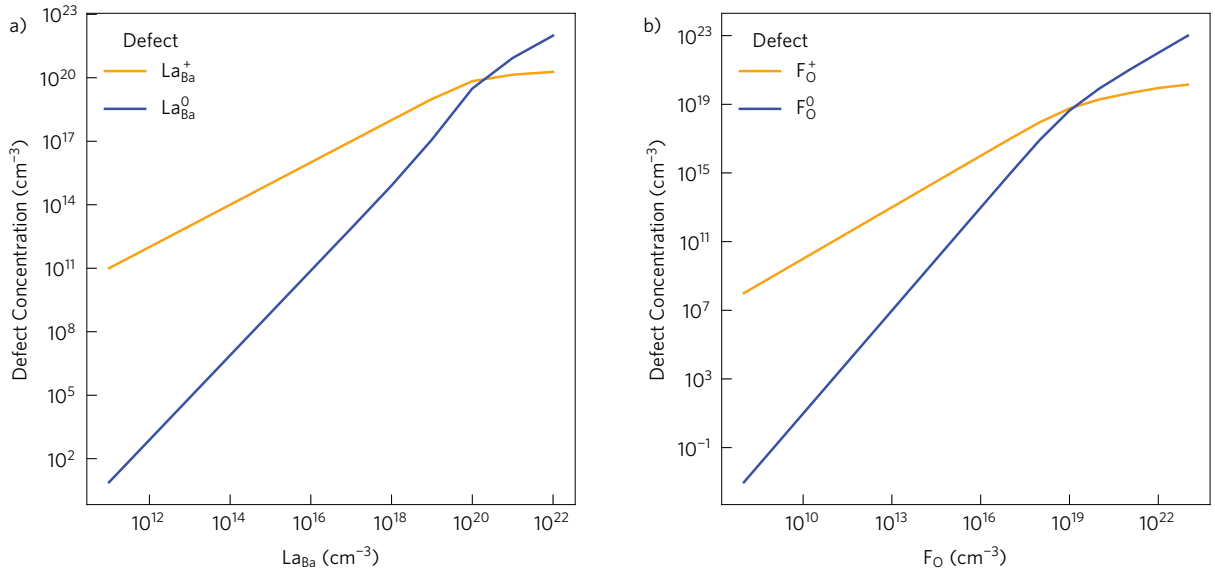

Figure S4: Concentrations of the different charge states for (a) La_{Ba} and (b) F_O in $BaBi_2O_6$. The x-axis value shows the total dopant amount that would be needed to get the carrier concentration given by the orange line. At high carrier concentrations, these values differ because a significant number of dopant atoms form neutral defects (blue line).

Oxygen Interstitial

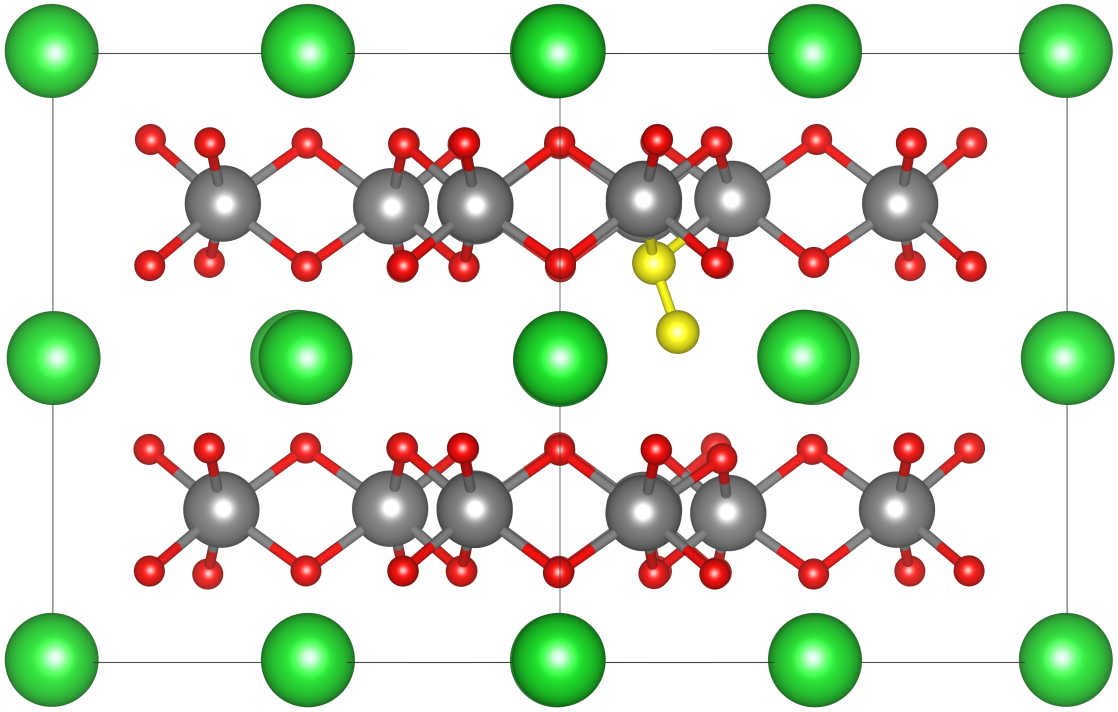

Figure S5: Relaxed O interstitial, which forms a peroxide-like species. Ba is green, Bi grey and O red, except for the peroxide-like defect in yellow.

AMSET inputs

Table S3: The k-point meshes used in the density of states (DoS), the interpolated DoS used in AMSET, density functional perturbation theory (DFPT) and optics calculations for $BaBi_2O_6$. The layers are in the ab plane. The high-frequency dielectric constant was calculated from the optics calculation, the ionic dielectric constant, elastic constant, piezoelectric constant (of 0) and polar optical phonon frequency were calculated from DFPT. The static dielectric constant is the sum of the high-frequency and ionic dielectric constants.

Calculation	DoS	Interpolated DoS	DFPT	Optics
k-point mesh	$12 \times 12 \times 12$	$91 \times 91 \times 75$	$14 \times 14 \times 12$	$10 \times 10 \times 9$

$$\text{High-frequency dielectric constant } (\epsilon_0) = \begin{bmatrix} 6.90 & 0 & 0 \\ 0 & 6.90 & 0 \\ 0 & 0 & 6.25 \end{bmatrix}$$

$$\text{Static dielectric constant } (\epsilon_0) = \begin{bmatrix} 17.26 & 0 & 0 \\ 0 & 17.18 & 0 \\ 0 & 0 & 9.79 \end{bmatrix}$$

$$\text{Elastic constant (GPa)} = \begin{bmatrix} 173 & 11 & 82 & 0 & 0 & 79 \\ 11 & 174 & 82 & 0 & 0 & -79 \\ 82 & 82 & 80 & 0 & 0 & 0 \\ 0 & 0 & 0 & 82 & -79 & 0 \\ 0 & 0 & 0 & -79 & 180 & 0 \\ 79 & -79 & 0 & 0 & 0 & 108 \end{bmatrix}$$

Polar optical phonon frequency (THz) = 8.70

Mobility

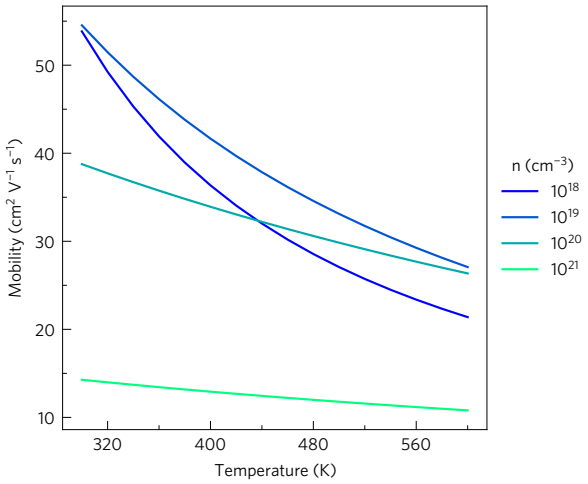

Figure S6: Electron mobility in the in-plane direction against temperature at various doping concentrations.

References

(1) Aroyo, M. I.; Orobengoa, D.; de la Flor, G.; Tasci, E. S.; Perez-Mato, J. M.; Wondratschek, H. Brillouin-Zone Database on the Bilbao Crystallographic Server. *Acta Crystallogr. A* **2014**, *70*, 126.

(2) Bradley, C.; Cracknell, A. *The Mathematical Theory of Symmetry in Solids: Representation Theory for Point Groups and Space Groups*; Oxford University Press, 2009.